Pertanika J. Sci. & Technol. 32 (2): 883 - 900 (2024)

PERTANIKA JOURNALS

SCIENCE & TECHNOLOGY

Journal homepage: http://www.pertanika.upm.edu.my/

Optimal Constrained Groove Pressing Process Parameters Applying Modified Taguchi Technique and Multi-Objective Optimization

Muni Tanuja Anantha[1,2]*, Sireesha Koneru[1], Saritha Pyatla[2], Parameshwaran Pillai Thiruvambalam Pillai[3], Tanya Buddi[4] and Nageswara Rao Boggarapu[1]

[1]Department of Mechanical Engineering, Koneru Lakshmaiah Education Foundation, Green Fields, Vaddeswaram, Guntur-522502, Andhra Pradesh, India

[2]Department of Mechanical Engineering, ANURAG University, Ghatkesar, Hyderabad-500088, Telangana, India

[3]Department of Mechanical Engineering, University College of Engineering, BIT Campus, Tiruchirappalli-620 024, Tamil Nadu, India

[4]Department of Mechanical Engineering, GRIET, Bachupally, Kukatpally, Hyderabad-500090, Telangana, India

ABSTRACT

Most engineering problems are complicated, and developing mathematical models for such problems requires understanding the phenomena through experiments. It is well known that as processing parameters with assigned levels increase, so does the number of experiments. By minimizing the number of experiments, Taguchi's method of experimental design will help to furnish the idea of full factorial experimental design. Taguchi's method is more appropriate for single-objective optimization problems and needs modifications while dealing with multi-objective optimization problems. Aluminum alloys are in great demand in today's automotive and aerospace sectors due to their low density, good corrosion resistance, and excellent machinability. The material is subjected to a constrained groove pressing (CGP) process to obtain microstructural grain refinement with enhanced mechanical behavior. This paper considers AA6061 material having major alloys such as silicon and magnesium. For this work, 3 CGP process parameters (viz., displacement rate, plate thickness and number of passes) are assigned 3 levels to each parameter, acquired the test data, viz., grain size (g_s), micro hardness (h_s), and tensile strength (σ_{ult}) based on L_9 orthogonal array of Taguchi.

ARTICLE INFO

Article history:
Received: 22 May 2023
Accepted: 09 October 2023
Published: 26 March 2024

DOI: https://doi.org/10.47836/pjst.32.2.21

E-mail addresses:
thanu.dhanu@gmail.com (Muni Tanuja Anantha)
sireekonerus@gmail.com (Sireesha Koneru)
sarithamech@anurag.edu.in (Saritha Pyatla)
paramesh551@yahoo.com (Parameshwaran Pillai Thiruvambalam Pillai)
tanyab@griet.ac.in (Tanya Buddi)
bnrao52@kluniversity.in (Nageswara Rao Boggarapu)
* Corresponding author

ISSN: 0128-7680
e-ISSN: 2231-8526

Using a modified version of Taguchi's methodology, it is possible to estimate the range of grain size (g_s), micro hardness (h_s), and tensile strength (σ_{ult}) for effective combinations of the CGP processing parameters and validate the results with existing test data. A more dependable and simpler multi-objective optimization procedure is used to choose the optimal CGP processing parameters.

Keywords: AA6061, displacement rate, grain size, micro hardness, number of passes, plate thickness, tensile strength

INTRODUCTION

The ability of the severe plastic deformation technique to successfully reduce the microstructure to nanoscale levels has attracted much attention in the fields of material science and engineering (Segal, 1995; Cherukuri & Srinivasan, 2006). Constrained groove pressing (CGP) and Accumulative roll bonding (ARB) are the two primary SPD techniques that are typically used to produce nanostructured sheets (Tsuji et al., 2003; Omotoyinbo & Oladele, 2010). Shin et al. (2002) provided the first detailed explanation of the CGP process, which includes multiple corrugating and flattening phases. During CGP, the work sample undergoes cyclic shear deformation using flat and asymmetrically grooved dies. In this method, an inclined section of the workpiece between the grooves undergoes pure shear deformation because the thickness of the work sample and the distance between the upper and lower dies are similar (Horita et al., 2001; Akin & Fedai, 2018). Figure 1 represents the detailed procedure of the CGP process. By including more CGP passes, the workpiece is subjected to higher stresses. Aluminum, Low 'C' steel, and copper alloys, when subjected to CGP, demonstrated considerable improvements in sheet metal's mechanical characteristics, as well as microstructural alterations (Lowe & Valiev, 2004; Kurzydłowski et al., 2004). The potentiality of processing using SPD for different the composites' special patterns was noted, and Equal channel angular pressing (ECAP), High-Pressure Torsion (HPT), Multi-axial forging (MAF), and additional SPD methods were examined (Kulagin et al., 2019; Husaain et al., 2017). The SPD methods were used to continuously draw low-carbon steel (Zavdoveev et al., 2021).

Using SPD techniques, ultra-fine grain structured metals and alloys have been created (Sauvage et al., 2012). The early stages of SPD development included HPT and ECAP processing methods (Sabirov et al., 2013). Later, a variety of SPD techniques were created, like ARB (accumulative roll bonding), CHPT (continuous high-pressure torsion), RCS (repeated corrugation and straightening), and CGP procedures (Khodabakhshi et al., 2011; Saritha et al., 2020). For sheet metals, ECAP, RCS, ARB, and CGP techniques are used (Mueller & Mueller, 2007; Saritha et al., 2018; Hu et al., 2018). Repeated corrugating and flattening phases are part of CGP. Specimens are highly strained by enforcing more CGP

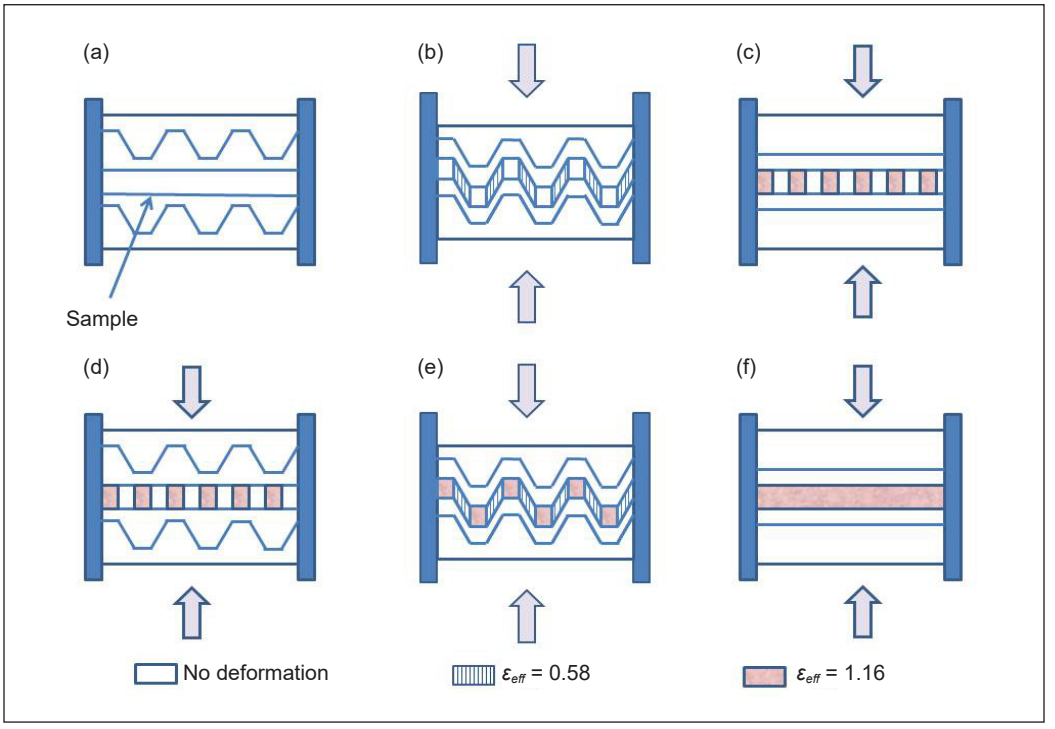

Figure 1. Detailed illustration of the CGP process

passes (Nazari & Honarpisheh, 2018). Several investigations were made on materials undergoing CGP (Nazari & Honarpisheh, 2019; Khodabakhshi et al., 2010; Kumar & Vedrtnam, 2021). Post-deformation annealing and cryo-rolling of Al-Mg alloys undergoing the CGP process enhanced the strength, ductility, and fracture toughness (Tanuja et al., 2022; Khandani et al., 2020). To determine the optimal die geometry (like the angle of the groove, the width of the groove, and the friction coefficient), a modified Taguchi technique with the data from the elastoplastic finite element analysis was used (Anantha et al., 2023a; Anantha et al., 2023b; Sahiti et al., 2017). Engineering optimization problems are solved using the Taguchi technique (Siddesha & Shantharaja, 2014; Rao et al., 2008; Singaravelu et al., 2009; Parameshwaranpillai et al., 2011). The strain homogeneity and the impact of processing parameters are examined using various techniques (Bharathi et al., 2016; Kumar, 2017; Ross, 1989; Pillai et al., 2018).

A hybrid experimental-numerical method was adopted for designing a suitable die through the groove pressing-cross route process (Googarchin et al., 2019; Hayes, 2000). An artificial neural network (ANN) and a two-objective genetic algorithm (GA) are used to seek an optimal solution (Ghorbanhosseini & Fereshteh-saniee, 2019). Girish et al. (2019) used AA6061 material with magnesium and silicon as major alloying elements. They considered displacement rate ($\dot{\delta}$), plate thickness (t) and number of passes (v_p) as

the 3 process parameters and assigned 3 levels to each parameter. They conducted 27 experiments for the possible combination of three process parameters and three assigned levels and reported the grain size (g_s), micro hardness (h_s) and tensile strength (σ_{ult}) measurements. Taguchi grey relational analysis was performed on the measured data to identify the optimal set of process variables that leads to ultra-fine grain structure with better mechanical characteristics.

For the 3 process parameters and the assigned 3 levels to each parameter, Taguchi's design of experiments recommends an L_9 orthogonal array (OA) to conduct 9 tests and obtain optimal solutions. The Taguchi method is well suited for optimizing a single objective output response and requires modifications to handle the problems of multi-objective output responses. This paper utilizes a modified approach of Taguchi with the simple technique of multi-objective optimization considering the data of 9 tests as per the L_9 OA to obtain the optimal solution and the estimated range of responses (g_s, h_s, σ_{ult}) for all 27 combinations of processing parameters ($\dot{\delta}$, v_p, t). Empirical relationships are developed and validated for g_s, h_s and σ_{ult} in terms of $\dot{\delta}$, t and v_p.

MATERIALS AND METHODS

Girish et al. (2019) conducted tests on AA 6061 (whose mechanical properties and chemical composition are given in Table 1) to select a set of optimal process parameters $\dot{\delta}$, v_p, t for improving the mechanical properties (g_s, h_s, σ_{ult}) of the sheet metal through the CGP process. Most researchers used Minitab as a computational tool and under-utilized the potential of Taguchi's experiment design. For the 3 process parameters with 3 levels, Taguchi's L_9 OA is appropriate for obtaining optimal solutions and generating the data of output responses for all the possible 27 sets of process parameters. A modified Taguchi approach is followed here to generate the complete information from the 9 tests and also the expected range of output responses. A simple multi-objective optimization procedure is presented to trace the optimal process parameters.

Table 1
Mechanical properties and chemical composition of the material

Mechanical Properties								
Young's modulus (GPa)						68		
Yield strength (MPa)						145		
Tensile strength (MPa)						241		
Hardness (HV)						107		
Poisson's ratio						0.33		
Chemical composition								
Element	Magnesium	Silicon	Copper	Chromium	Zinc	Manganese	Titanium	Aluminum
wt %	0.93	0.62	0.28	0.17	0.21	0.06	0.10	Bal

Analysis

In order to improve the mechanical properties, the process parameters need to be combined optimally; three levels are assigned to each experimental parameter, as represented in Table 2. The displacement rate ($\dot{\delta}$) varies from 1 to 2 mm/min, and the thickness (t) ranges from 3 to 5 mm, with the number of passes (v_p) varying from 1 to 5.

Table 2
Levels assigned to the experimental parameters

Input Parameters	1st Level	2nd Level	3rd Level
Displacement rate, $\dot{\delta}$ (mm/min)	1	1.5	2
Number of passes, v_p	1	3	5
Thickness, t (mm)	3	4	5
Fictitious, ε	ε_1	ε_2	ε_3

Table 3 shows the L_9 orthogonal array of Taguchi, which is considered for three parameters of the experimentation process ($N_p = 3$), each assigned with three levels ($N_l = 3$) using Equation 1 (Ross, 1989) to reduce the 27 possible combinations of the process parameters.

$$N_{Tag} = 1 + N_p \times (N_l = 3 - 1) \quad [1]$$

According to Equation 1, $N_{Tag} = 7$, and the optimal solution results for a set of 9 test data are presented in Table 3. $N_{Tag} = 9$; $N_p = 4$ and $N_l = 3$. As in (Dharmendra et al., 2019 Dharmendra et al., 2020 Satyanarayana et al., 2021), a fictitious parameter (ε) is presented in Table 2.

In Table 3, the experimental findings for grain size (g_s), hardness (h_s), and tensile strength (σ_{ult}) have been presented. The outcomes of ANOVA are presented in Table 4. The findings demonstrate that the number of passes (v_p) had a maximum impact on grain size (g_s) as well as on hardness (h_s), with a contribution of 87.2% and 79.7%, respectively. Thickness (t) greatly influences tensile strength (σ_{ult}), contributing 51.9%. The contribution of $\dot{\delta}$ and t on g_s are 3.6% and 8.6%, respectively, whereas 4.6% and 15% for h_s and 0.2% and 46.6% for σ_{ult}. Total % contributions of $\dot{\delta}$, t and v_p and ε is 100. The % error of the grand mean of the output responses is considered as the % contribution of the parameter ε.

Modified Taguchi method (Dharmendra et al., 2019; Dharmendra et al., 2020; Satyanarayana et al., 2021) can provide the estimate range for the mechanical properties (viz., grain size 'g_s', micro hardness 'h_s' and tensile strength 'σ_{ult}') for the specified set of process parameters as input variables viz., displacement rate ($\dot{\delta}$), number of passes (v_p) and thickness (t), which will help design the process to know the possible scatter for the repeated experiments. On representing $\widehat{\phi}$ as a performance indicator and applying the additive law (Ross, 1989), $\widehat{\phi}$ is predicted for the levels of the process parameters from Equation 2.

Table 3
Mechanical properties, viz., grain size (g_s), tensile strength (σ_{ult}) and micro hardness (h_s), having levels of the parameters as per L_9 OA (orthogonal array)

Test Run	Parameter levels				Mechanical properties		
	$\dot{\delta}$	v_p	t	ε	g_s (μm)	h_s (HV)	σ_{ult} (MPa)
1	1	1	1	1	7.7	44.48	94.820
2	1	2	2	2	6.4	45.50	109.81
3	1	3	3	3	4.0	47.98	96.000
4	2	1	2	3	7.2	44.38	96.920
5	2	2	3	1	5.0	45.45	91.100
6	2	3	1	2	4.2	52.78	114.70
7	3	1	3	2	6.4	42.33	78.690
8	3	2	1	3	6.3	47.91	104.51
9	3	3	2	1	3.8	52.23	121.94
Grand mean					5.667	47.004	100.943

Table 4
Findings from Analysis of Variance (ANOVA) regarding mechanical properties (g_s, h_s, and σ_{ult})

Input Parameters	1st Mean	2nd Mean	3rd Mean	SOS (Sum of squares)	Contribution (%)
Grain size, g_s (μm)					
$\dot{\delta}$	6.033	5.466	5.500	0.606	3.60
v_p	7.100	5.900	4.000	14.66	87.2
t	6.066	5.800	5.133	1.386	8.20
ε	5.500	5.667	5.833	0.166	1.00
Micro hardness, h_s (HV)					
$\dot{\delta}$	45.986	47.536	47.490	4.664	4.60
v_p	43.730	46.286	50.996	81.53	79.7
t	48.390	47.370	45.253	15.36	15.0
ε	47.386	46.870	46.756	0.676	0.70
Tensile strength, σ_{ult} (MPa)					
$\dot{\delta}$	100.210	100.906	101.713	3.3960	0.20
v_p	90.143	101.806	110.880	648.36	46.6
t	104.676	109.556	88.596	721.70	51.9
ε	102.620	101.066	99.143	18.199	1.30

$$\hat{\phi} = \bar{\phi}_g + \sum_{i=1}^{n_p} \left(\bar{\phi}_i - \bar{\phi}_g\right) = \sum_{i=1}^{n_p} \bar{\phi}_i - \left(n_p - 1\right)\bar{\phi}_g \quad [2]$$

$\bar{\phi}_i$ is the mean value of ϕ from the table of the ANOVA for the 'i' level of process parameters, and $\bar{\phi}_g$ is referred to as the grand mean of ϕ for experimental runs. The subscript 'i' = 1, 2, 3, and 4, in this case, stands for $\dot{\delta}$, t, v_p, ε, respectively. The test results are compared to the estimates of 'g_s', 'h_s', and 'σ_{ult}' as shown in Table 5 for the nine test

runs of Taguchi's L_9 orthogonal array. In Equation 2, the variables $N_p = 4$ and $N_p = 3$ provide estimates for g_s, h_s and σ_{ult} with fictitious parameter (ε). Taguchi method considers $N_p = 3$ to identify the optimal set of process parameters from the levels of optimal mean values in the ANOVA table and to estimate the output response using the additive law (Equation 2).

Equation 2 can be used to determine the range of estimates with the consideration of maximum and minimum mean values of 'g_s', 'h_s' and 'σ_{ult}' and for 'ε'. The mechanical property estimates in Table 5 using 'ε' (i.e., $N_p = 4$ in Equation 2) have an exact match with the test results, whereas Taguchi's method with $N_p = 3$ in Equation 2 showed deviation from the test data. For the various levels of $\dot{\delta}$, v_p and t, the corrections for g_s with estimates are -0.166 and 0.167 μm; the corrections for h_s estimates are -0.248 and 0.382 HV; and the corrections for σ_{ult} estimates are -1.8 and 1.68 MPa. The test results in Tables 5 to 7 are within/close to the estimated range of g_s, h_s and σ_{ult}.

Table 5
Comparison of test data with estimates of grain size, g_s (μm) for AA6061

Test Run	Parameter levels				Test	Estimate Equation 2			Estimated range	
	$\dot{\delta}$	v_p	t	ε		$N_p = 3$	R.E. (%)	$N_p = 4$	Lower- bound	Upper- bound
1	1	1	1	1	7.7	7.866	-2.2	7.7	7.700	8.033
2	1	2	2	2	6.4	6.400	0.0	6.4	6.233	6.566
3	1	3	3	2	4.0	3.833	4.2	4.0	3.666	4.000
4	2	1	2	3	7.2	7.033	2.3	7.2	6.866	7.200
5	2	2	3	1	5.0	5.166	-3.3	5.0	5.000	5.333
6	2	3	1	2	4.2	4.200	0.0	4.2	4.033	4.366
7	3	1	3	2	6.4	6.400	0.0	6.4	6.233	6.566
8	3	2	1	3	6.3	6.133	2.6	6.3	5.966	6.300
9	3	3	2	1	3.8	3.966	-4.4	3.8	3.800	4.133

Table 6
Comparison of test data with estimates of micro hardness, h_s (HV) for AA6061

Test Run	Parameter levels				Test	Estimate Equation 2			Estimated range	
	$\dot{\delta}$	v_p	t	ε		$N_p = 3$	R.E. (%)	$N_p = 4$	Lower- bound	Upper- bound
1	1	1	1	1	44.48	44.098	0.9	44.48	43.850	44.480
2	1	2	2	2	45.50	45.634	-0.3	45.50	45.387	46.017
3	1	3	3	2	47.98	48.228	-0.5	47.98	47.980	48.610
4	2	1	2	3	44.38	44.628	-0.6	44.38	44.380	45.010
5	2	2	3	1	45.45	45.068	0.8	45.45	44.820	45.450
6	2	3	1	2	52.78	52.914	-0.3	52.78	52.667	53.297
7	3	1	3	2	42.33	42.464	-0.3	42.33	42.217	42.847
8	3	2	1	3	47.91	48.158	-0.5	47.91	47.910	48.540
9	3	3	2	1	52.23	51.848	0.9	52.33	51.60	52.230

Table 7
Comparison of test data with obtained estimates for tensile strength, σ_{ult} (MPa) for AA6061

Test Run	Parameter levels				Test	Estimate Equation 2			Estimated range	
	$\dot{\delta}$	v_p	t	ε		$N_p = 3$	R.E. (%)	$N_p = 4$	Lower- bound	Upper- bound
1	1	1	1	1	94.820	93.143	1.8	94.820	91.340	94.81
2	1	2	2	2	109.81	109.69	0.1	109.81	107.89	111.4
3	1	3	3	2	96.000	97.800	-1.9	96.000	96.000	99.47
4	2	1	2	3	96.920	98.720	-1.9	96.920	96.920	100.4
5	2	2	3	1	91.100	89.423	1.7	91.000	87.620	91.09
6	2	3	1	2	114.70	114.58	0.1	114.70	112.78	116.2
7	3	1	3	2	78.690	78.567	0.2	78.690	76.770	80.23
8	3	2	1	3	104.51	106.31	-1.7	104.51	104.51	108.0
9	3	3	2	1	121.94	120.26	1.4	121.94	118.46	121.9

Nine test runs are performed in accordance with Taguchi's L_9 OA approach; Equation 2 assigns the estimates of g_s, h_s, and σ_{ult} for all 27 combinations of input variables viz., displacement rate ($\dot{\delta}$), number of passes (v_p) and thickness (t). These 27 input variable combinations are arranged sequentially $(\dot{\delta}_i, \nu_{pj}, t_k), k = 1\ to\ 3), j = 1\ to\ 3), i = 1\ to\ 3)$. The sequence numbers (1,5,9,11,15,16,21,22,26) represent the 9 test runs considered in the L_9 orthogonal array of Taguchi represented in Table 3. Test outcomes of the work (Girish et al., 2019) and the generated lower and upper bounds of g_s, h_s, and σ_{ult} from Equation 2 are displayed in Figures 2(a) to 2(c).

Taking into account the mean values of ANOVA in Table 4 for g_s, h_s and σ_{ult}, the constructed empirical relations using input variables ($\dot{\delta}$, v_p and t) are as in Equations 3 to 5.

$$g_s = 5.8333 - 0.26667\xi_1 + 0.3\xi_1^2 - 1.55\xi_2 - 0.35\xi_2^2 - 0.4667\xi_3 - 0.2\xi_3^2 \quad [3]$$

$$h_s = 47.1844 + 0.751667\xi_1 - 0.79833\xi_1^2 + 3.63333\xi_2 + 1.076667\xi_2^2 - 1.56833\xi_3 - 0.54833\xi_3^2 \quad [4]$$

$$\sigma_{ult} = 110.3833 + 0.751667\xi_1 + 0.055\xi_1^2 + 10.36833\xi_2 - 1.295\xi_2^2 - 8.04\xi_3 - 12.92\xi_3^2 \quad [5]$$

Here, $\xi_1 = 2\dot{\delta} - 3$; $\xi_2 = 0.5\nu_p - 1.5$; and $\xi_3 = t - 4$.

Applying Equation 2 and the constructed empirical Equations 3 to 5, the estimates of g_s, h_s and σ_{ult} shown in Figures 3(a) to 3(c) provide a good comparison. The estimated lower bound of g_s, h_s and σ_{ult} are attained by making corrections -0.1667μm, -0.248 HV, and -1.8MPa to g_s, h_s and σ_{ult} in Equations 3 to 5, the application of corrections yields upper bound estimates as 0.167 μm, 0.382 HV and 1.68MPa in Equations 3 to 5.

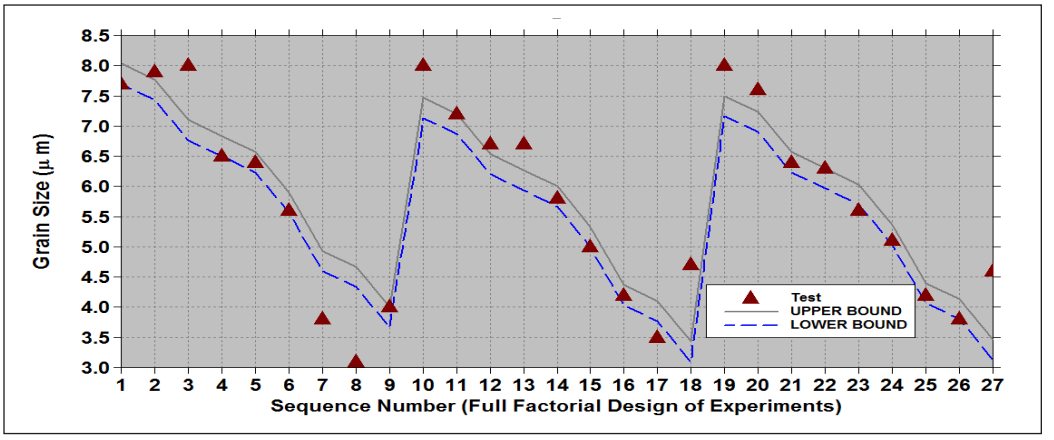

(a)

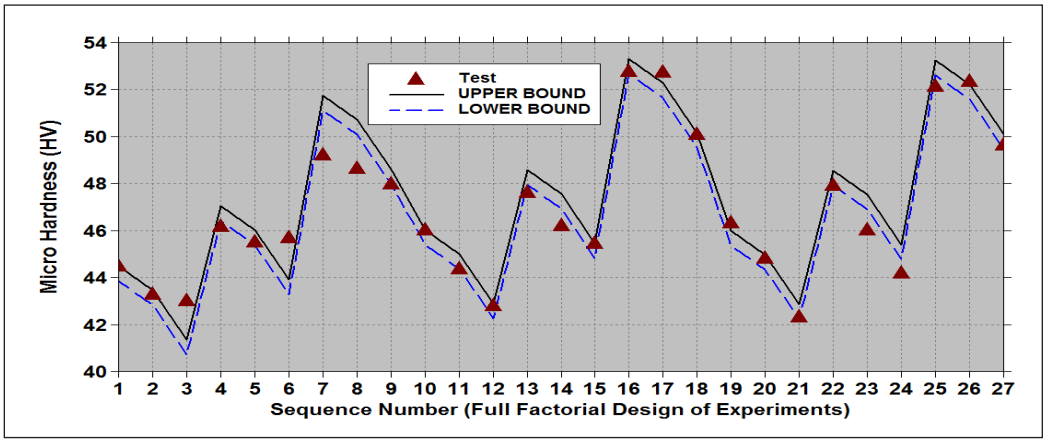

(b)

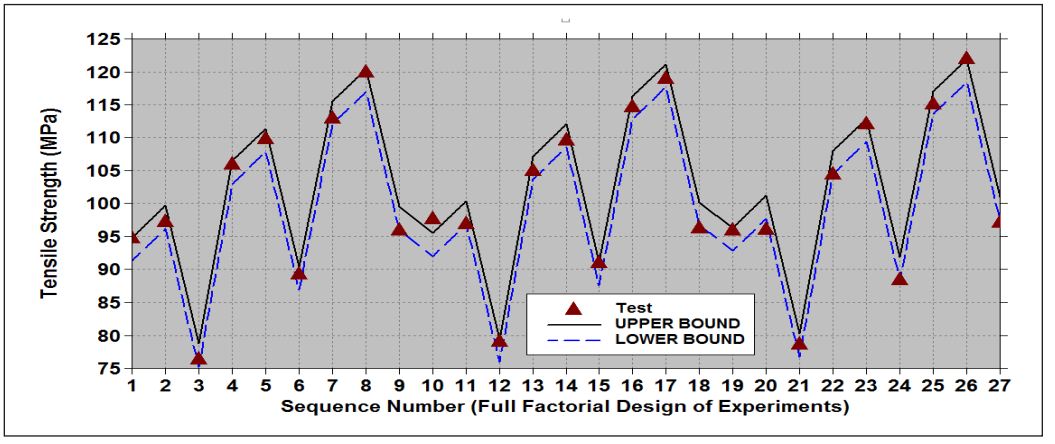

(c)

Figure 2. (a) Estimates of grain size, g_s (μm) for AA6061with test data (Girish et al., 2019); (b) Estimates of micro hardness, h_s (HV) for AA6061with test data (Girish et al., 2019); (c) Estimates of tensile strength, σ_{ult} (MPa) for AA6061with test data (Girish et al., 2019)

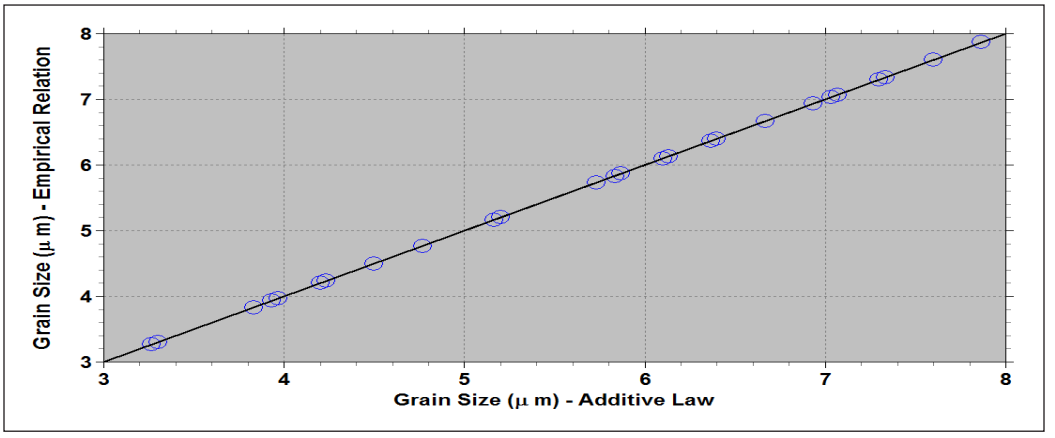

(a)

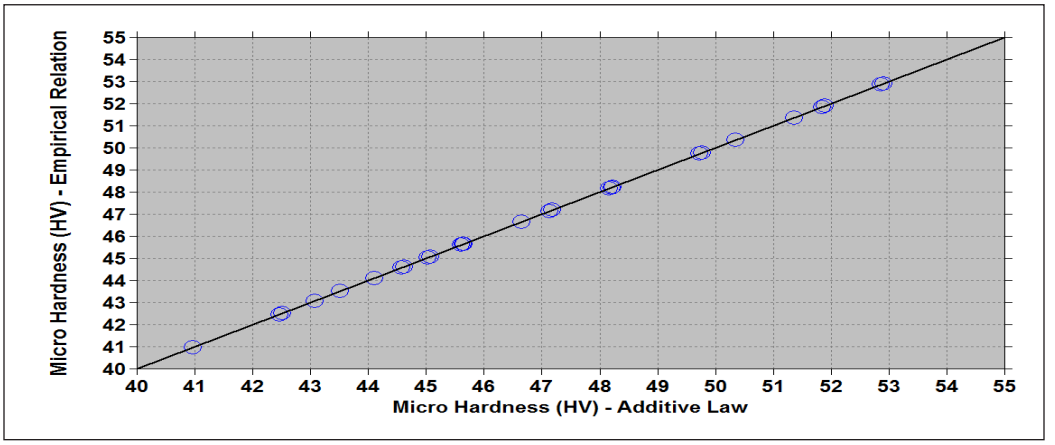

(b)

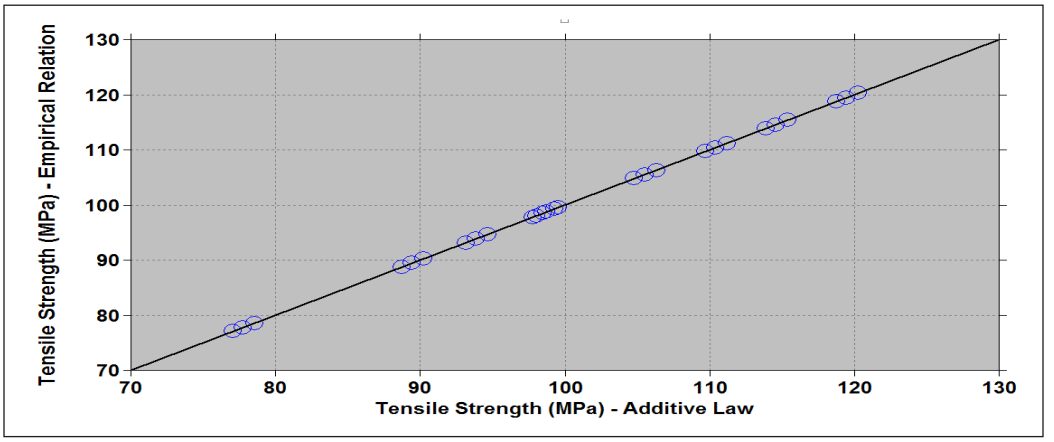

(c)

Figure 3. (a) Comparison of estimates of grain size g_s (μm) using Equations 2 and 3, (b) Comparison of estimates of micro hardness, h_s (HV)for AA6061 using Equations 2 and 4, (c) Comparison of estimates of tensile strength, σ_{ult} (MPa) for AA6061using the Equations 2 and 5

RESULTS AND DISCUSSION

Optimal Solution

For achieving the minimum grain size (g_s), a set of input parameters ($\dot{\delta}_2\ v_{p3}\ t_3$) (where the level of the input variable is indicated by subscripts) are listed in ANOVA Table 4. A different set of parameters ($\dot{\delta}_2\ v_{p3}\ t_1$) was identified for achieving maximum micro hardness (h_s). Another set of parameters ($\dot{\delta}_3\ v_{p3}\ t_1$) was identified for achieving maximum tensile strength (σ_{ult}). Table 8 gives the output responses viz., grain size (g_s), micro hardness (h_s), and tensile strength (σ_{ult}) for the various input variable optimal sets that have been found. To obtain the minimum grain size (g_s), maximum micro hardness (h_s), and maximum tensile strength (σ_{ult}), a multi-objective optimization analysis can be used to determine the best set of optimal input variables.

For single-objective optimization problems, the Taguchi method is more appropriate (Mohamed et al., 2015). In the case of multiple responses optimization, the utility concept based on Taguchi is utilized (Tong et al., 1997; Gaitonde et al., 2009; Akin & Fedai, 2018; Lonavath & Boda, 2023; Anantha et al., 2023a). Applying Taguchi method concepts, a reliable multi-objective optimization technique has been used. This approach defines a single function ζ with weighing factors (ω_1, ω_2 and ω_3, which satisfies $\omega_1 + \omega_2 + \omega_3 = 1$) and the output responses (g_s, h_s and σ_{ult}) in Equation 6.

$$\zeta = \omega_1\left(\frac{g_s}{g_{s\,\max}}\right) + \omega_2\left(1 - \frac{h_s}{h_{s\,\max}}\right) + \omega_3\left(1 - \frac{\sigma_{ult}}{\sigma_{ult\ \max}}\right) \quad [6]$$

Table 8
Output responses for the identified optimal set of input variables through single objective optimization

Input Variables				Output Responses		
Optimal Set	Displacement rate, '$\dot{\delta}$' (mm/min)	Number of passes, 'v_p'	Thickness, 't' (mm)	Grain size, 'g_s' (μm)	Micro hardness, 'h_s' (HV)	Tensile strength, 'σ_{ult}' (MPa)
In the case of minimum grain size, g_s						
$\dot{\delta}_2\ v_{p3}\ t_3$	1.5	5	5	3.1–3.433 (4.7)+	49.53 – 50.16 (50.08)	96.7–100.2 (96.25)
In the case of maximum micro hardness, h_s						
$\dot{\delta}_2\ v_{p3}\ t_1$	1.5	5	3	4.0333–4.36667 (4.2)	52.667–53.297 (52.78)	112.78–116.2 (114.7)
In the case of maximum tensile strength, σ_{ult}						
$\dot{\delta}_3\ v_{p3}\ t_1$	2	5	3	4.0667 –4.4 (4.2)	52.62–53.25 (52.13)	113.58–117.1 (115.18)

Note. + Results in parenthesis are from tests

Minimization of ζ provides the minimum g_s, maximum h_s and σ_{ult} assigning equal weighing factors to a set of input variables: $\omega_1 = \omega_2 = \omega_3 = 1/3$. Here, $g_{s\,max} = 8.033$ μm; $h_{s\,max} = 53.297$ HV; and $\sigma_{ult\,max} = 121.94$ MPa. Values of ζ are produced using the data in Table 3 and presented the data in Table 9. ANOVA is carried out on ζ as given in Table 10.

To achieve the minimum ζ, the optimal input variables are $\dot{\delta}_2\ v_{p3}\ t_2$. This optimal set of input variables corresponds to a displacement rate of 1.5 mm/min; number of passes as 5; and sheet thickness as 4 mm. The range of output responses for the optimal input variables, as determined by Equations 3 to 5 are: grain size, g_s = 3.76 – 4.1 μm; micro hardness, h_s = 51.647 – 52.277 HV, and the tensile strength, σ_{ult} = 117.66 – 121.1MPa. The test results for the optimal input variables are as follows: grain size =3.5 μm; and tensile strength = 119.01 MPa and micro hardness = 52.73 HV. The % Contribution of the number of passes on the grand mean of the output responses is high. Figures 4(a) to 4(c) illustrate the variation of output responses depending on the number of passes for the ideal input variables, displacement rate = 1.5 mm/min, and thickness = 4 mm.

Table 9
Single objective function (ζ) in Equation 6 from the mechanical properties, viz., grain size (g_s), micro hardness (h_s) and tensile strength (σ_{ult}) with levels of the process parameters based on L_9 OA (orthogonal array)

Test Run	Parameter levels			Normalized output responses			Objective function, ζ
	$\dot{\delta}$	v_p	t	$\frac{g_s}{g_{s\max}}$	$1-\frac{h_s}{h_{s\max}}$	$1-\frac{\sigma_{ult}}{\sigma_{ult\max}}$	Eq.(6)
1	1	1	1	0.95850	0.19821	0.28601	0.48091
2	1	2	2	0.79668	0.17135	0.11046	0.35950
3	1	3	3	0.49792	0.11081	0.27021	0.29298
4	2	1	2	0.89626	0.20092	0.25815	0.45177
5	2	2	3	0.62240	0.17264	0.33853	0.37786
6	2	3	1	0.52282	0.00978	0.06312	0.19857
7	3	1	3	0.79668	0.25907	0.54962	0.53513
8	3	2	1	0.78423	0.11243	0.16678	0.35448
9	3	3	2	0.47302	0.02042	0	0.16448

Table 10
Results of ANOVA on the single objective function, from ζ Table 9

Input parameters	1st Mean	2nd Mean	3rd Mean
$\dot{\delta}$	0.377798	**0.342738**	0.351364
v_p	0.489272	0.363947	**0.218681**
t	0.344657	**0.325254**	0.401989

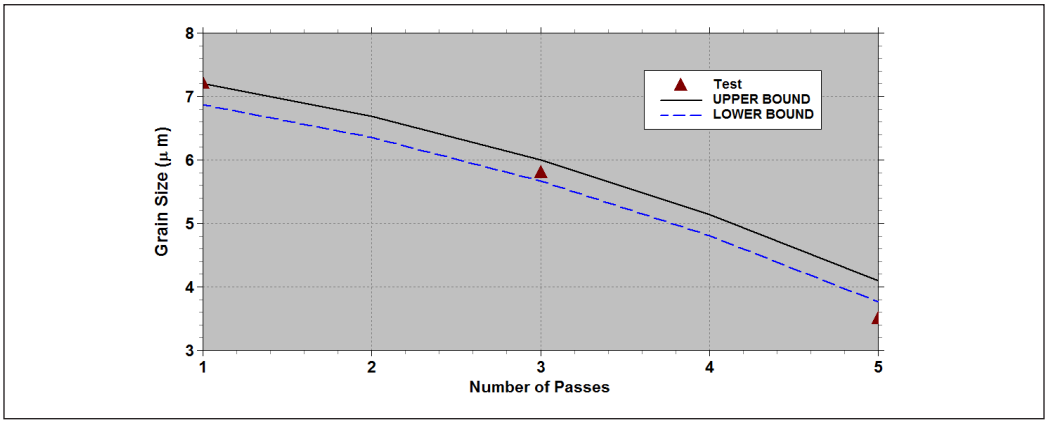

(a)

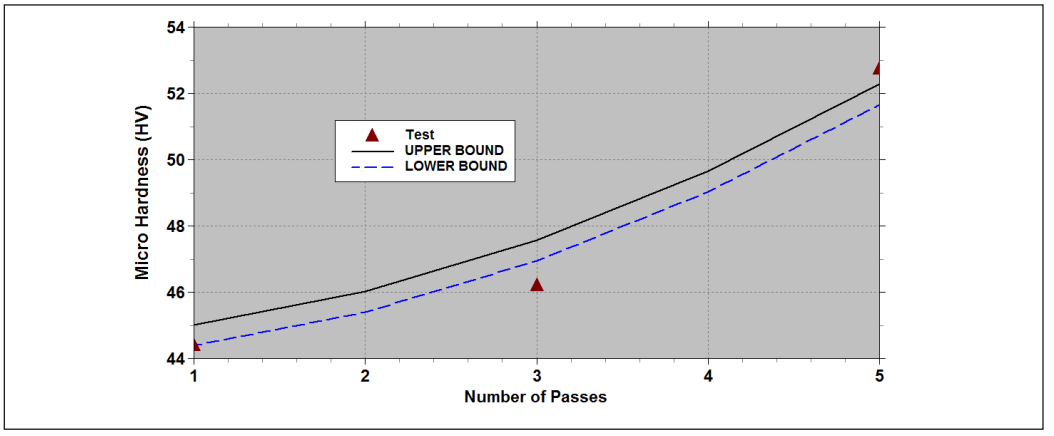

(b)

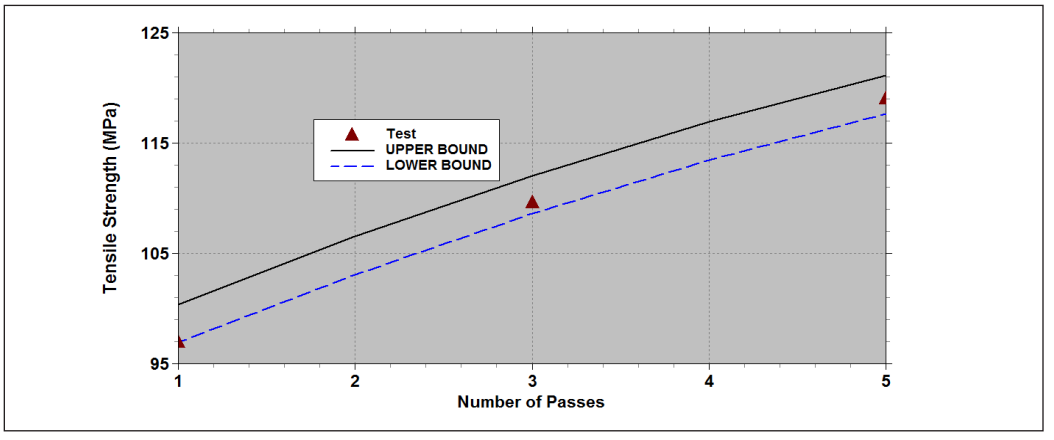

(c)

Figure 4. (a) Grain size versus number of passes for the optimal input variables, displacement rate = 1.5 mm/min; and thickness = 4 mm; (b) Micro hardness versus number of passes for the optimal input variables, displacement rate = 1.5 mm/min; and thickness = 4 mm; (c) Tensile strength versus number of passes for the optimal input variables, displacement rate = 1.5 mm/min; and thickness = 4 mm

CONCLUSION

Aluminum alloys are in high demand in the aerospace and automobile sectors because of their low density, high resistance to corrosion and machinability. The mechanical properties can be improved by refining the grain structure using constrained groove pressing (CGP).

Developing mathematical models for such complex problems needs experimentation to understand the phenomena. However, it is known that the time-consuming experiments will be expensive due to the requirement of large numbers by increasing the processing parameters with assigned levels. Modified Taguchi's design of experiments with a simple multi-objective optimization procedure adopted in this study to obtain optimal process parameters with a minimum number of experiments and the data with expected range for the full factorial design of experiments—empirical relationships developed and validated for the output responses in terms of process parameters for AA6061.

The mechanical properties of AA6061 were enhanced by refining the grain structure using CGP. Taguchi's L_9 orthogonal array (OA) is selected for the 3 CGP process parameters (viz., displacement rate, $\dot{\delta}$; plate thickness, t; and number of passes, v_p) and assigned 3 levels to each parameter. ANOVA analysis was performed from the acquired data (viz., grain size, g_s; micro hardness, h_s; and tensile strength, σ_{ult}) of 9 tests. The % contribution of each CGP parameter is evaluated on the grand mean of g_s, h_s and σ_{ult}. Following are the highlights of the present study.

- ANOVA results indicate that a number of passes (v_p) has a maximum influence on grain size (g_s) with a contribution of 87.2% and on micro hardness (h_s) with a contribution of 79.7%, whereas thickness (t) has a maximum impact on tensile strength (σ_{ult}) having a contribution of 51.9%.
- The displacement rate is 1.5mm/min; the number of passes is 5 and the thickness is 5mm, which are the optimal CGP process variables to achieve minimum grain size (g_s).
- The displacement rate is 1.5mm/min; the number of passes is 5, and the thickness is 3mm, which are the optimal CGP process variables to achieve maximum micro hardness (h_s).
- The displacement rate is 2mm/min; the number of passes is 5, and the thickness is 3mm, which are the optimal CGP process variables to achieve maximum tensile strength (σ_{ult}).
- The displacement rate is 1.5mm/min; the number of passes is 5, and the thickness of 4 mm is the optimal CGP process variable to achieve minimum grain size (g_s), maximum micro hardness (h_s), and maximum tensile strength (σ_{ult}).

ACKNOWLEDGEMENTS

The authors thank the Koneru Lakshmaiah Education Foundation, Green Fields, Vaddeswaram, Guntur-522502, Andhra Pradesh, India, for providing the facility to carry out the research study. The authors are also grateful to the handling editor and the reviewers for their valuable comments, which helped improve the quality of this manuscript.

REFERENCES

Akin, H. K., & Fedai, Y. (2018). Optimization of machining parameters in face milling using multi-objective Taguchi technique. *Tehnički Glasnik, 12*(2), 104-108. https://doi.org/10.31803/tg-20180201125123

Anantha, M. T., Buddi, T., & Boggarapu, N. R. (2023a). Multi-objective optimization basing modified Taguchi method to arrive the optimal die design for CGP of AZ31 magnesium alloy. *International Journal on Interactive Design and Manufacturing*, 1-10. https://doi.org/10.1007/s12008-022-01176-6

Anantha, M. T., Buddi, T., & Boggarapu, N. R. (2023b). Utilisation of fuzzy logic and genetic algorithm to seek optimal corrugated die design for CGP of AZ31 magnesium alloy. *Advances in Materials and Processing Technologies*, 1-15. https://doi.org/10.1080/2374068X.2023.2192135

Bharathi, P., Priyanka, T. G. L., Rao, G. S., & Rao, B. N. (2016). Optimum WEDM process parameters of SS304 using taguchi method. *International Journal of Industrial and Manufacturing Systems Engineering*, *1*(3), 69-72.

Cherukuri, B., & Srinivasan, R. (2006). Properties of AA6061 processed by multi-axial compressions/ forging (MAC/F). *Materials and Manufacturing Processes, 21*(5), 519-525. https://doi.org/10.1080/10426910500471649

Dharmendra, B. V., Kodali, S. P., & Rao, B. N. (2019). A simple and reliable Taguchi approach for multi-objective optimization to identify optimal process parameters in nano-powder-mixed electrical discharge machining of INCONEL800 with copper electrode. *Heliyon, 5*(8), Article e02326. https://doi.org/10.1016/j.heliyon.2019.e02326

Dharmendra, B. V., Kodali, S. P., & Boggarapu, N. R. (2020). Multi-objective optimization for optimum abrasive water jet machining process parameters of Inconel718 adopting the Taguchi approach. *Multidiscipline Modeling in Materials and Structures, 16*(2), 306-321. https://doi.org/10.1108/MMMS-10-2018-0175

Gaitonde, V. N., Karnik, S. R., & Davim, J. P. (2009). Multiperformance optimization in turning of free-machining steel using taguchi method and utility concept. *Journal of Materials Engineering and Performance, 18*(3), 231-236. https://doi.org/10.1007/s11665-008-9269-6

Ghorbanhosseini, S., & Fereshteh-saniee, F. (2019). Multi-objective optimization of geometrical parameters for constrained groove pressing of aluminium sheet using a neural network and the genetic algorithm. *Journal of Computational Applied Mechanics, 50*(2), 275-281. https://doi.org/10.22059/jcamech.2018.267948.335

Girish, B. M., Siddesh, H. S., & Satish, B. M. (2019). Taguchi grey relational analysis for parametric optimization of severe plastic deformation process. *SN Applied Sciences, 1*(8). https://doi.org/10.1007/s42452-019-0982-6

Googarchin, H. S., Teimouri, B., & Hashemi, R. (2019). Analysis of constrained groove pressing and constrained groove pressing-cross route process on AA5052 sheet for automotive body structure applications. *Proceedings of the Institution of Mechanical Engineers, Part D: Journal of Automobile Engineering, 233*(6), 1436-1452. https://doi.org/10.1177/0954407018785734

Hayes, J. S. (2000). Effect of grain size on tensile behaviour of a submicron grained Al-3 wt-%Mg alloy produced by severe deformation. *Materials Science and Technology, 16*(11-12), 1259-1263. https://doi.org/10.1179/026708300101507479

Horita, Z., Fujinami, T., & Langdon, T. G. (2001). The potential for scaling ECAP: Effect of sample size on grain refinement and mechanical properties. *Materials Science and Engineering A, 318*(1-2), 34-41. https://doi.org/10.1016/S0921-5093(01)01339-9

Hu, H., Qin, X., Zhang, D., & Ma, X. (2018). A novel severe plastic deformation method for manufacturing AZ31 magnesium alloy tube. *International Journal of Advanced Manufacturing Technology, 98*(1-4), 897-903. https://doi.org/10.1007/s00170-018-2179-3

Husaain, Z., Ahmed, A., M. Irfan, O., & Al-Mufadi, F. (2017). Severe plastic deformation and its application on processing titanium: A review. *International Journal of Engineering and Technology, 9*(6), 626-431. https://doi.org/10.7763/ijet.2017.v9.1011

Khandani, S. T., Faraji, G., & Torabi, H. (2020). Development of a new integrated severe plastic deformation method. *Materials Science and Technology, 36*(4), 468-476. https://doi.org/10.1080/02670836.2019.1710926

Khodabakhshi, F., Kazeminezhad, M., & Kokabi, A. H. (2010). Constrained groove pressing of low carbon steel: Nano-structure and mechanical properties. *Materials Science and Engineering A, 527*(16-17), 4043-4049. https://doi.org/10.1016/j.msea.2010.03.005

Khodabakhshi, F., Kazeminezhad, M., & Kokabi, A. H. (2011). Mechanical properties and microstructure of resistance spot welded severely deformed low carbon steel. *Materials Science and Engineering A, 529*(1), 237-245. https://doi.org/10.1016/j.msea.2011.09.023

Kulagin, R., Beygelzimer, Y., Bachmaier, A., Pippan, R., & Estrin, Y. (2019). Benefits of pattern formation by severe plastic deformation. *Applied Materials Today, 15*, 236-241. https://doi.org/10.1016/j.apmt.2019.02.007

Kumar, D. R. (2017). Optimum drilling parameters of coir fiber-reinforced polyester composites. *American Journal of Mechanical and Industrial Engineering, 2*(2), 92-97. https://doi.org/10.11648/j.ajmie.20170202.15

Kumar, S., & Vedrtnam, A. (2021). Experimental and numerical study on effect of constrained groove pressing on mechanical behaviour and morphology of aluminium and copper. *Journal of Manufacturing Processes, 67*, 478-486. https://doi.org/10.1016/j.jmapro.2021.05.008

Kurzydłowski, K. J., Garbacz, H., & Richert, M. (2004). Effect of severe plastic deformation on the microstructure and mechanical properties of Al and Cu. *Reviews on Advanced Materials Science, 8*(2), 129-133.

Lonavath, S. N., & Boda, H. (2023). Consequences of the rotational speed and profile of tool pin in microstructure and mechanical properties of AA8011/ZrO_2 composite produced by FSW. *International Journal on Interactive Design and Manufacturing*, 1-13. https://doi.org/10.1007/s12008-023-01295-8

Lowe, T. C., & Valiev, R. Z. (2004). The use of severe plastic deformation techniques in grain refinement. *JOM, 56*(10), 64-68. https://doi.org/10.1007/s11837-004-0295-z

Mohamed, M. A., Manurung, Y. H. P., & Berhan, M. N. (2015). Model development for mechanical properties and weld quality class of friction stir welding using multi-objective Taguchi method and response surface methodology. *Journal of Mechanical Science and Technology, 29*(6), 2323-2331. https://doi.org/10.1007/s12206-015-0527-x

Mueller, K., & Mueller, S. (2007). Severe plastic deformation of the magnesium alloy AZ31. *Journal of Materials Processing Technology, 187-188*, 775-779. https://doi.org/10.1016/j.jmatprotec.2006.11.153

Nazari, F., & Honarpisheh, M. (2018). Analytical model to estimate force of constrained groove pressing process. *Journal of Manufacturing Processes, 32*, 11-19. https://doi.org/10.1016/j.jmapro.2018.01.015

Nazari, F., & Honarpisheh, M. (2019). Analytical and experimental investigation of deformation in constrained groove pressing process. *Proceedings of the Institution of Mechanical Engineers, Part C: Journal of Mechanical Engineering Science, 233*(11), 3751-3759. https://doi.org/10.1177/0954406218809738

Omotoyinbo, J. A., & Oladele, I. O. (2010). The effect of plastic deformation and magnesium content on the mechanical properties of 6063 aluminium alloys. *Journal of Minerals and Materials Characterization and Engineering, 09*(06), 539-546. https://doi.org/10.4236/jmmce.2010.96038

Parameshwaranpillai, T., Lakshminarayanan, P. R., & Rao, B. N. (2011). Taguchi's approach to examine the effect of drilling induced damage on the notched tensile strength of woven GFR-epoxy composites. *Advanced Composite Materials, 20*(3), 261-275. https://doi.org/10.1163/092430410X547083

Pillai, J. U., Sanghrajka, I., Shunmugavel, M., Muthuramalingam, T., Goldberg, M., & Littlefair, G. (2018). Optimisation of multiple response characteristics on end milling of aluminium alloy using Taguchi-Grey relational approach. *Measurement: Journal of the International Measurement Confederation, 124*, 291-298. https://doi.org/10.1016/j.measurement.2018.04.052

Rao, B. S., Rudramoorthy, R., Srinivas, S., & Rao, B. N. (2008). Effect of drilling induced damage on notched tensile and pin bearing strengths of woven GFR-epoxy composites. *Materials Science and Engineering A, 472*(1-2), 347-352. https://doi.org/10.1016/j.msea.2007.03.023

Ross, P. J. (1989). *Taguchi techniques for quality engineering*. McGraw-Hill.

Sabirov, I., Murashkin, M. Y., & Valiev, R. Z. (2013). Nanostructured aluminium alloys produced by severe plastic deformation: New horizons in development. *Materials Science and Engineering A, 560*, 1-24. https://doi.org/10.1016/j.msea.2012.09.020

Sahiti, M., Reddy, M. R., Joshi, B., & Rao, B. N. (2017). Application of taguchi method for optimum weld process parameters of pure aluminum. *American Journal of Mechanical and Industrial Engineering, 1*(3), 123-128. https://doi.org/10.11648/j.ajmie.20160103.25

Saritha, P., Raju, P. R., Reddy, R. V., & Snehalatha, S. (2018). Mechanical behavior of hybrid composites. *International Journal of Mechanical Engineering and Technology, 9*(9), 71-76.

Saritha, P., Satyadevi, A., & Raju, P. R. (2020). Tribological behavior of metal matrix composites. *Journal of Advanced Research in Dynamical and Control Systems, 12*(2), 2335-2341. https://doi.org/10.5373/JARDCS/V12I2/S20201280

Satyanarayana, G., Narayana, K. L., & Rao, B. N. (2021). Incorporation of Taguchi approach with CFD simulations on laser welding of spacer grid fuel rod assembly. *Materials Science and Engineering B: Solid-State Materials for Advanced Technology, 269*, Article 115182. https://doi.org/10.1016/j.mseb.2021.115182

Sauvage, X., Wilde, G., Divinski, S. V., Horita, Z., & Valiev, R. Z. (2012). Grain boundaries in ultrafine grained materials processed by severe plastic deformation and related phenomena. *Materials Science and Engineering A, 540*, 1-12. https://doi.org/10.1016/j.msea.2012.01.080

Segal, V. M. (1995). Materials processing by simple shear. *Materials Science and Engineering A, 197*(2), 157-164. https://doi.org/10.1016/0921-5093(95)09705-8

Shin, D. H., Park, J. J., Kim, Y. S., & Park, K. T. (2002). Constrained groove pressing and its application to grain refinement of aluminum. *Materials Science and Engineering A, 328*(1), 98-103. https://doi.org/10.1016/S0921-5093(01)01665-3

Siddesha, H. S., & Shantharaja, M. (2014). Optimization of cyclic constrained groove pressing parameters for tensile properties of Al6061/sic metal matrix composites. *Procedia Materials Science, 5*, 1929-1936. https://doi.org/10.1016/j.mspro.2014.07.515

Singaravelu, J., Jeyakumar, D., & Rao, B. N. (2009). Taguchi's approach for reliability and safety assessments in the stage separation process of a multistage launch vehicle. *Reliability Engineering and System Safety, 94*(10), 1526-1541. https://doi.org/10.1016/j.ress.2009.02.017

Tanuja, A. M., Kumar, A., & Rao, B. N. (2022). Review on the application of CGP to improve AZ31 Mg alloy properties. In *Applications of Computational Methods in Manufacturing and Product Design: Select Proceedings of IPDIMS 2020* (pp. 237-246). Springer Nature. https://doi.org/10.1007/978-981-19-0296-3_21

Tong, L. I., Su, C. T., & Wang, C. H. (1997). The optimization of multi-response problems in the Taguchi method. *International Journal of Quality and Reliability Management, 14*(4), 367-380. https://doi.org/10.1108/02656719710170639

Tsuji, N., Saito, Y., Lee, S. H., & Minamino, Y. (2003). ARB (accumulative roll-bonding) and other new techniques to produce bulk ultrafine grained materials. *Advanced Engineering Materials, 5*(5), 338-344. https://doi.org/10.1002/adem.200310077

Zavdoveev, A., Baudin, T., Pashinska, E., Kim, H. S., Brisset, F., Heaton, M., Poznyakov, V., Rogante, M., Tkachenko, V., Klochkov, I., & Skoryk, M. (2021). Continuous severe plastic deformation of low-carbon steel: Physical-mechanical properties and multiscale structure analysis. *Steel Research International, 92*(3), Article 2000482. https://doi.org/10.1002/srin.202000482